Max-Planck-Institut
für Polymerforschung

Max Planck Institute
for Polymer Research

DNA–Polymer Conjugates by Photoinduced RAFT Polymerization

Thorsten Lueckerath, Tina Strauch, Kaloian Koynov, Christopher Barner-Kowollik*, David Y. W. Ng* and Tanja Weil*

DNA-Polymer Conjugates by Photo-induced RAFT Polymerization

Thorsten Lueckerath,[1] Tina Strauch,[1] Kaloian Koynov,[1] Christopher Barner-Kowollik,[2,3]* David Ng,[1]* Tanja Weil[1]*

[1] Max Planck Institute for Polymer Research, Ackermannweg 10, 55128 Mainz (Germany)

[2] School of Chemistry, Physics and Mechanical Engineering, Queensland University of Technology (QUT), George Street, QLD 4000, Brisbane (Australia)

[3] Macromolecular Architectures, Institut für Technische Chemie und Polymerchemie, Karlsruhe Institute of Technology (KIT), Engesserstraße 18, 76131 Karlsruhe (Germany)

Abstract: Conventional grafting-to approaches to DNA-polymer conjugates are often limited by low reaction yields due to the sterically hindered coupling of a pre-synthesized polymer to DNA. The grafting-from strategy, in contrast, allows to directly graft polymers from an initiator that is covalently attached to DNA. Herein, we report blue light-mediated reversible addition-fragmentation chain-transfer (Photo-RAFT) polymerization from two different RAFT agent-terminated DNA sequences using Eosin Y as the photocatalyst in combination with ascorbic acid. Three monomer families (methacrylates, acrylates and acrylamides) were successfully

polymerized from DNA employing Photo-RAFT polymerization. We demonstrate that the length of the grown polymer chain can be varied by altering the monomer to DNA-initiator ratio, while the self-assembly features of the DNA strands were maintained. In summary, we describe a convenient, light-mediated approach towards DNA-polymer conjugates *via* the grafting-from approach.

Introduction

The combination of synthetic polymers with the unique specificity and recognition properties of DNA gave rise to an all-new class of DNA-polymer hybrid materials.[1–5] In recent years, DNA-polymer conjugates have emerged as versatile building blocks that provided enhanced stability to complex DNA nanostructures[6,7] or facilitated, e.g., the precise organization of polymeric structures by DNA.[8–12] In particular, the combination of DNA with a hydrophobic polymer chain resulted in amphiphilic species that formed supramolecular architectures such as micelles or vehicles.[13–15] These assemblies were intensively investigated in the context of drug delivery,[16–19] as scaffolds for directing organic reactions[20] or as virus-like particles.[21] Inspired by recent advances in designing more sophisticated 2D and 3D DNA architectures equipped with various functionalities,[22,23] polymer chains were organized within complex DNA scaffolds or grown from DNA origami templates in distinct nanostructures.[24,25]

Until recently, grafting-to strategies of pre-synthesized polymers to DNA sequences were mainly accomplished following solid phase synthesis[13,20,26,27] or bioconjugation strategies, such as copper-mediated azide-alkyne,[28,29] thiol-ene,[30–32] amide[33–35] or recently also tetrazine-norbornene coupling.[36] While the major advantage related to both approaches is that the polymer can be thoroughly characterized prior to the coupling reaction, the nature of the polymer has to be

carefully selected, e. g., it must remain stable under the strongly basic conditions of DNA-cleavage from the solid support. Critically, variation of polymer lengths to, i.e., improve stability and bioactivity is more tedious *via* the grafting-to strategy and low reaction yields were reported.[32,37] Most likely, steric hindrance of the pre-formed polymer chain or the necessity to use organic solvents during the conjugation step caused problems, particularly when hydrophobic, high molecular weight polymers were employed.[36]

Therefore, grafting-from polymerization from the DNA sequence containing the covalently attached initiator would be highly desirable for achieving DNA-polymer conjugates. Compared to the grafting-to strategy, grafting-from polymerization offers more convenient purification and higher coupling yields. Here, reversible-deactivation radical polymerizations[38] such as atom transfer radical polymerization (ATRP)[39,40] or RAFT polymerization[41,42] are often favoured due to their exceptional characteristics in terms of non-demanding reaction conditions, high control over molecular weight, molecular weight distribution (MWD) and end-group functionality.

First grafting-from approaches from DNA sequences immobilized on different surfaces following either ATRP or RAFT polymerization have been reported.[43–47] However, no particular insights in understanding the polymerization process from DNA were given and only limited characterization of the resulting DNA-polymer conjugates was provided as they mostly remained at the surface. Matyjaszewski and co-workers significantly contributed by providing full analytics on the composition of DNA-polymer conjugates synthesized *via* conventional ATRP as well as photoATRP directly in solution.[48,49]

ATRP methods that rely on toxic transition metal catalysts have several limitations as catalysts are challenging to remove from the polyanionic DNA-polymer conjugates. However, important progress in metal-free ATRP has been made recently,[50–52] which offers key future potential for

achieving DNA-polymer conjugates. RAFT polymerization does typically not require metal catalysts and, in addition, offers similar flexibility in terms of monomer scope and end-group functionalization.[53] In particular, recent developments in photo-induced RAFT polymerizations – particularly the introduction of photo-induced electron transfer (PET)-RAFT polymerization by Boyer and co-workers[54–56] – allow initiating the RAFT process solely by irradiating a biocompatible dye with visible light.[57] Therefore, the RAFT approach provides an elegant polymerization platform particularly for biological systems such as cells or proteins.[58,59]

We believe that photo-induced RAFT (Photo-RAFT) polymerizations will substantially enlarge the polymer chemist's toolset for the synthesis of DNA-polymer conjugates, yet it has, to the best of our knowledge, not been exploited for the grafting-from preparation of DNA-polymer conjugates freely in solution. Herein, we report the solution-based Photo-RAFT polymerization from two RAFT agent-terminated single-stranded DNA (RAFT-ssDNA) sequences, which were derived from the established RAFT agents 4-cyano-4-(phenylcarbonothioylthio)pentanoic acid (CPADB) and 2-(butylthiocarbonothioyl)propionic acid (BTPA). Methacrylates, acrylates and acrylamides were applied as monomers for blue light-mediated RAFT polymerization. A series of new ssDNA-polymer conjugates of varying monomers and chain lengths were achieved while the DNA terminus remained functionally intact throughout the course of polymerization. In summary, we provide a powerful and robust grafting-from method in solution by light activation that offers many opportunities for achieving tailored DNA-polymer conjugates.

Experimental

Materials. 2-Bromopropionic acid (Alfa Aesar, 98 %), 1-butanethiol (Fluka, >97 %), carbon disulphide (Acros Organics, 99,9 %), 4-cyano-4-(phenylcarbonothioylthio)pentanoic acid (CPADB, 99,9 %), *N,N'*-diisopropylcarbodiimide (DIC, Sigma, 99 %), *N,N*-diisopropylethylamine (DIPEA, Roth, >99,5 %), *N*-(3-dimethylaminopropyl)-*N'*-ethylcarbodiimide hydrochloride (EDC*HCl, Sigma, 98 %), 4-dimethylaminopyridine (DMAP, Sigma, >99 %), 3-hydroxypicolinic acid (Sigma, >99 %), *N*-hydroxysuccinimide (NHS, Sigma, 98 %), pentafluorophenol (PFP, Merck, >99 %), organic solvents (VWR), dry solvents (Sigma, 99,8 %), deuterated solvents (Sigma or Deutero GmbH, 99,9 %) and silica gel 60 (Macherey-Nagel GmbH) were all used as received. The nucleotides for DNA synthesis were purchased from Link Technologies Ltd. Amine-terminated ssDNA was either self-synthesized by using a commerically available C6 amino modifier from Glen Research or purchased from Sigma or biomers.net. All other functional DNAs used within this study were purchased from biomers.net. Poly(ethylene glycol) methyl ether methacrylate (Sigma, M_n = 300 g/mol, stabilized with 100 ppm MeHQ and 300 ppm BHT), poly(ethylene glycol) methyl ether acrylate (Sigma, M_n = 480 g/mol, stabilized with 100 ppm MeHQ and 100 ppm BHT) and *N,N*-dimethylacrylamide (Acros Organics, stabilized with 500 ppm MeHQ) were passed through a short column of alumina prior to use. *N-Iso*propylacrylamide (NIPAM, Sigma, 97 %) was recrystallized twice from a 1 to 1 mixture of toluene and pentane. The blue LED array lamp (item number: LIU470a) was purchased from Thorlabs, Inc.

Synthesis of 2-(((butylthio)carbonothioyl)thio)propanoic acid (BTPA). BTPA was synthesized according to a literature procedure with slight changes.[1] Briefly, 1-butanethiole (1.67 mL, 1.40 g, 15.5 mmol, 1.00 eq.) and carbon disulphide (1.02 mL, 1.30 g, 17.1 mmol, 1.10 eq.) were stirred in

1 M NaOH (17 mL) for 1 hour. The reaction mixture was cooled to 0 °C and a solution of 1-bromopropionic acid (2.61 g, 17.1 mmol, 1.10 eq.) in 1 M NaOH (17 mL) was slowly added. After stirring overnight, the aqueous phase was overlaid with cyclohexane and acidified to pH = 1 with concentrated hydrochloric acid solution. The organic phase was collected, dried over magnesium sulphate and concentrated *in vacuo*. Recrystallization from cyclohexane gave the clean product as a yellow solid after storage in the fridge (1.80 g, 7.55 mmol, 49 %). ^{1}H NMR (300 MHz, DMSO-d_6): δ(ppm) = 13.17 (brs, 1H), 4.68 (q, J = 7.3 Hz, 1H), 3.45-3.28 (m, 2H), 1.70-1.56 (m, 2H), 1.51 (d, J = 7.3 Hz, 3H), 1.44-1.27 (m, 2H), 0.89 (t, J = 7.3 Hz, 3H). ^{13}C NMR (125 MHz, DMSO-d_6): δ(ppm) = 222.9, 172.0, 48.6, 36.7, 30.1, 21.9, 17.2, 13.9. ESI-MS: Calc.: [M+H]$^+$ = 239.38, found: [M+H]$^+$ = 239.

Synthesis of BTPA-NHS. BTPA-NHS was synthesized according to a literature procedure with slight changes.[2] BTPA (250 mg, 1.05 mmol, 1.00 eq.), NHS (117 mg, 1.15 mmol, 1.10 eq.) and DMAP (12.8 mg, 105 μmol, 0.10 eq.) were added to dry DMF (10 mL). The mixture was cooled to 0 °C and EDC*HCl (261 mg, 1.36 mmol, 1.30 eq.) was slowly added as a solid. After stirring overnight, the reaction mixture was diluted with DCM (30 mL), washed with brine (3x) and dried over sodium sulphate. Concentration *in vacuo* gave a yellow liquid as the crude product, which had to be further purified using column chromatography (CH/EA = 2:1). The final product was obtained as a yellow viscous oil (156 mg, 0.46 mmol, 46 %). ^{1}H NMR (300 MHz, DMSO-d_6): δ(ppm) = 5.13 (q, J = 7.4 Hz, 1H), 3.41 (t, J = 7.3 Hz, 2H), 2.80 (s, 4H), 1.72-1.57 (m, 5H), 1.45-1.30 (m, 2H), 0.89 (t, J = 7.3 Hz, 3H). ^{13}C NMR (125 MHz, DMSO-d_6): δ(ppm) = 221.0, 170.3, 167.7, 45.4, 37.0, 30.0, 26.0, 21.9, 16.6, 13.9. ESI-MS: Calc.: [M+Na]$^+$ = 358.44, found: [M+Na]$^+$ = 358.

Synthesis of BTPA-PhF5. BTPA-PhF5 was synthesized according to a literature procedure with slight changes.[2] Briefly, BTPA (200 mg, 0.84 mmol, 1.00 eq.), PFP (263 mg, 1.43 mmol, 1.70 eq.) and DMAP (10.3 mg, 84.0 μmol, 0.10 eq.) were added to dry DCM (10 mL.) The mixture was cooled to 0 °C and a solution of DIC (260 μL, 212 mg, 1.68 mmol, 2.00 eq.) in dry DCM (10 mL) was added dropwise. After stirring overnight, the precipitate was filtered off and the reaction mixture was concentrated *in vacuo*. Column chromatography (CH/EA = 9:1) gave the final product as a yellow liquid (227 mg, 0.56 mmol, 67 %). ^{1}H NMR (300 MHz, CD$_2$Cl$_2$): δ(ppm) = 5.02 (q, J = 7.4 Hz, 1H), 3.32 (t, J = 7.3 Hz, 2H), 1.72-1.56 (m, 5H), 1.43-1.28 (m, 2H), 0.89 (t, J = 7.3 Hz, 3H). ^{19}F NMR (470 MHz, DMSO-d$_6$): δ(ppm) = -152.2 (d, J = 20.8 Hz, 2F), -157.4 (t, J = 21.6 Hz, 1F), -162.0 (t, 21.1 Hz, 2F) ESI-MS: Calc.: [M+H]$^+$ = 405.43, found: [M+H]$^+$ = 405.

Synthesis of CPADB-NHS. CPADB (300 mg, 1.07 mmol, 1.00 eq.), NHS (136 mg, 1.18 mmol, 1.10 eq.) and DMAP (13.1 mg, 107 μmol, 0.10 eq.) were dissolved in dry DCM (10 mL). The mixture was cooled to 0 °C and EDC*HCl (309 mg, 1.61 mmol, 1.50 eq.) was slowly added as a solid. After stirring overnight, the reaction mixture was diluted with DCM (30 mL) and washed with brine (1x), 1 M NaOH (2x) and 1 M HCl (2x). The organic phase was dried over magnesium sulphate and was concentrated *in vacuo* to afford a pink solid as the crude product. Further purification *via* column chromatography (CH/EA = 2:1) gave the final product as a pink powder (145 mg, 0.39 mmol, 36 %). ^{1}H NMR (300 MHz, DMSO-d$_6$): δ(ppm) = 7.98-7.92 (m, 2H), 7.74-7.66 (m, 1H), 7.56-7.48 (m, 2H), 3.14-2.90 (m, 2H), 2.83 (s, 4H), 2.75-2.56 (m, 2H), 1.96 (s, 3H). ^{13}C NMR (125 MHz, DMSO-d$_6$): δ(ppm) = 224.1, 170.6, 168.2, 144.4, 134.2, 129.5, 127.0, 118.9, 46.2, 31.8, 26.7, 25.9, 23.4. ESI-MS: Calc.: [M+H]$^+$ = 377.45, found: [M+H]$^+$ = 377.

Synthesis of CPADB-PhF$_5$. CPADB (250 mg, 0.89 mmol, 1.00 eq.), PFP (181 mg, 0.98 mmol, 1.10 eq.) and DMAP (10.9 mg, 89.2 µmol, 0.10 eq.) were added to dry DCM (10 mL.) The mixture was cooled to 0 °C and a solution of DIC (152 µL, 124 mg, 0.98 mmol, 1.10 eq.) in dry DCM (10 mL) was added dropwise. After stirring overnight, the precipitate was filtered off and the reaction mixture was concentrated *in vacuo*. Column chromatography (CH/EA = 10:1) gave the final product as a pink oil (119 mg, 0.27 mmol, 30 %). ^{1}H NMR (300 MHz, CD$_2$Cl$_2$): δ(ppm) = 7.89-7.82 (m, 2H), 7.57-7.48 (m, 1H), 7.39-7.32 (m, 2H), 3.02-2.95 (m, 2H), 2.74-2.44 (m, 2H), 1.90 (s, 3H). ^{19}F NMR (470 MHz, DMSO-d$_6$): δ(ppm) = -153.1 (d, J = 20.3 Hz, 2F), -158.5 (t, J = 21.8 Hz, 1F), -162.9 (t, J = 21.1 Hz, 2F). ESI-MS: Calc.: [M+H]$^+$ = 446.42, found: [M+H]$^+$ = 446.

Synthesis of NH$_2$-DNA. After DNA synthesis, the oligonucleotides were cleaved from the solid support by incubation with concentrated ammonia at ambient temperature for 16 hours. The MMT group was manually removed by following a standard protocol for MMT-deprotection of oligonucleotides.[3]

Synthesis of CPADB-DNA *via* NHS or PFP Coupling. NH$_2$-DNA (1.00 mg, 172 nmol, 1.00 eq.) at a concentration of 250 µM relative to the total amount of solvent, CPADB-NHS (3.23 mg, 8.58 µmol, 50.0 eq.) or CPADB-PhF$_5$ (3.82 mg, 8.58 nmol, 50.0 eq.), respectively, and DIPEA (0.60 µL, 0.44 mg, 3.43 µmol, 20.0 eq.) were shaken in a 1 to 1 mixture of DMF and nuclease-free water for 30 minutes. Residual CPADB-NHS was removed *via* centrifugation (5 min, 12500 rpm, 20 °C). The supernatant was evaporated and the residue was picked up in a 1 to 1 mixture of acetonitrile and water. The sample was then subjected to HPLC purification and the desired peak was collected between 11.74 min and 12.77 min. The fractions were combined, the solvent was

removed and the residue was picked up in nuclease-free water to determine the concentration (682 μg, 112 nmol, 65 %). For MALDI ToF mass spectra, the DNA was once precipitated from isopropanol to desalt the sample from the buffer salts of HPLC purification.

Synthesis of BTPA-DNA *via* NHS or PFP Coupling. NH$_2$-DNA (1.00 mg, 172 nmol, 1.00 eq.) at a concentration of 250 μM relative to the total amount of solvent, BTPA-NHS (2.88 mg, 8.58 μmol, 50.0 eq.) or BTPA-PhF$_5$ (3.47 mg, 8.58 μmol, 50.0 eq.), respectively, and DIPEA (0.60 μL, 0.44 mg, 3.43 μmol, 20.0 eq.) were shaken in a 1 to 1 mixture of DMF and nuclease-free water for 2 hours. The supernatant was evaporated and the residue was picked up in a 1 to 1 mixture of acetonitrile and water. The solution was then subjected to HPLC purification and the desired peak was collected between 12.30 min and 13.21 min. The fractions were combined, the solvent was removed and the residue was picked up in nuclease-free water to determine the concentration (835 μg, 138 nmol, 80 %). For MALDI ToF mass spectra, the DNA was once precipitated from isopropanol to desalt the sample from the buffer salts of HPLC purification.

Conventional Photo-RAFT Polymerization of Acrylamides and Acrylates. A typical experiment was conducted by charging a custom-built schlenk tube with DMA (2.06 μL, 1.98 mg, 20.0 μmol, 200 eq.), BTPA (23.9 μg, 0.10 μmol, 1.00 eq.), Eosin Y (6.48 μg, 0.01 μmol, 0.10 eq.), ascorbic acid (18.0 μg, 0.10 μmol, 1.00 eq.) and water (17.9 μL) as the solvent. The schlenk flask was properly sealed and degassed by freeze-pump-thaw (3 x). The tube was then placed in the photoreactor as shown above and irradiated by a blue LED ($\lambda_{max.}$ = 470 nm, 4 mW/cm^2) at room temperature. The samples were analyzed by GPC with DMF as the eluent in order to determine apparent molecular weights and dispersities.

Conventional Photo-RAFT Polymerization of Methacrylates. A typical experiment was conducted by charging a custom-built schlenk tube with OEGMA (5.71 μL, 6.00 mg, 20.0 μmol, 200 eq.), CPADB (27.9 μg, 0.10 μmol, 1.00 eq.), Eosin Y (6.48 µg, 0.01 µmol, 0.10 eq.), ascorbic acid (18.0 μg, 0.10 μmol, 1.00 eq.) and water (14.3 μL) as the solvent. The schlenk flask was properly sealed and degassed by freeze-pump-thaw (3 x). The tube was then placed in the photoreactor as shown above and irradiated by a blue LED ($\lambda_{max.}$ = 470 nm, 4 mW/cm^2) at room temperature. The samples were analyzed by GPC with DMF as the eluent in order to determine apparent molecular weights and dispersities.

Photo-RAFT Polymerization of Acrylamides and Acrylates from DNA. A typical experiment was conducted by charging a custom-built schlenk tube with DMA (2.06 μL, 1.98 mg, 20.0 μmol, 200 eq.), BTPA-DNA (605 μg, 0.10 μmol, 1.00 eq.), Eosin Y (6.48 μg, 0.01 µmol, 0.10 eq.), ascorbic acid (18.0 μg, 0.10 μmol, 1.00 eq.) and water (17.9 μL) as the solvent. The schlenk flask was properly sealed and degassed by freeze-pump-thaw (3 x). The tube was then placed in the photoreactor as shown above and irradiated by a blue LED ($\lambda_{max.}$ = 470 nm, 4 mW/cm^2) at room temperature. After a predetermined time interval, the polymerization was stopped by removing the light source and exposing to oxygen. The DNA-polymer conjugate was purified by membrane filtration (3 x, MWCO = 10 kDA) and was subsequently analyzed by GPC, native PAGE and FCS.

Photo-RAFT Polymerization of Methacrylates from DNA. A typical experiment was conducted by charging a custom-built schlenk tube with OEGMA (5.71 μL, 6.00 mg, 20.0 μmol, 200 eq.), CPADB-DNA (609 μg, 0.10 μmol, 1.00 eq.), Eosin Y (6.48 µg, 0.01 µmol, 0.10 eq.),

ascorbic acid (18.0 μg, 0.10 μmol, 1.00 eq.) and water (14.3 μL) as the solvent. The schlenk flask was properly sealed and degassed by freeze-pump-thaw (3 x). The tube was then placed in the photoreactor as shown above and irradiated by a blue LED ($\lambda_{max.}$ = 470 nm, 4 mW/cm^2) at room temperature. After a predetermined time interval, the polymerization was stopped by removing the light source and exposing to oxygen. The DNA-polymer conjugate was purified by membrane filtration (3 x, MWCO = 10 kDA) and was subsequently analyzed by GPC, native PAGE and FCS.

Results and Discussion

In automated DNA synthesis, the terminal functionality is generally introduced to ssDNA sequences by using phoshoramidite coupling chemistry.[60] This process requires incubation with concentrated ammonia for several hours, e.g., for DNA cleavage from the solid support, and the newly incorporated functionality has to remain stable under these harsh conditions. In contrast to ATRP initiators that have been attached to ssDNA sequences directly on the solid support,[48,49] RAFT agents are typically not stable in very basic media or in the presence of primary amines and they would thus decompose during cleavage from the solid support.[61–63] Therefore, two RAFT-ssDNA sequences (BTPA-DNA and CPADB-DNA) were achieved by conjugating the RAFT agent to the amine-terminated ssDNA sequence (NH$_2$-ssDNA) in solution and not *via* the phosphoramidite approach as depicted in Figure 1.
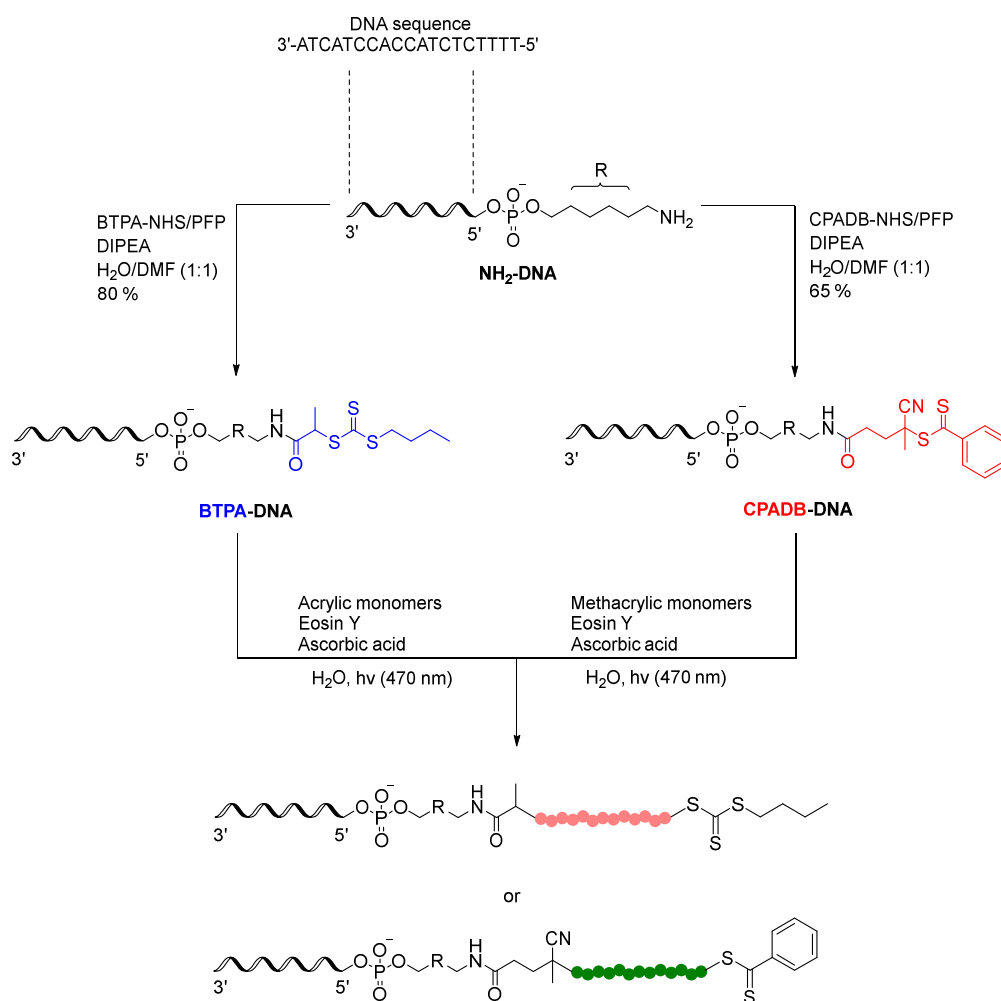
Figure 1. Schematic Overview on the Synthesis towards DNA-Polymer Conjugates by Photo-RAFT Polymerization.

Synthesis of the DNA-Photo-RAFT initiators

The conjugation of the RAFT agent to DNA was accomplished by amide conjugation as reported for RAFT polymerization from surface-anchored DNA before.[46,47] CPADB and BTPA were selected for controlling RAFT polymerizations of either methacrylic or acrylic monomers. The ligation was conducted by reacting 19-mer NH_2-ssDNA (3'-ATCATCCACCATCTCTTTT-5'-AminoC6) with the activated *N*-hydroxysuccinimide (NHS) or pentafluorophenyl (PFP) esters of

the two chosen RAFT agents in a mixture of water and DMF, which was necessary to ensure sufficient solubility of all reagents. Due to the competitive hydrolysis reaction in partly aqueous medium, the activated esters were added in large excess ($\geq$ 50 eq.) and in conjunction with *N*,*N*-di*iso*propylethylamine (DIPEA) as an auxiliary base in order to increase the reactivity of the amine moiety. Reaction control by HPLC indicated that less equivalents of the PFP ester were required to achieve higher conversions, presumably due to its higher hydrolytic stability when compared to the respective NHS ester.[64] Full conversion of the NH_2-DNA was achieved after 30 minutes for activated CPADB and after 2 hours for activated BTPA, respectively. In both reactions, a clear shift in the corresponding HPLC spectra (Figure 2) was observed during product formation. Slightly higher yields were obtained for activated BTPA (~ 80%) than for activated CPADB (~ 65 %), probably again due to the higher hydrolytic stability of the trithiocarbonate group compared to the dithiobenzoic acid moiety of CPADB. In contrast to the often low coupling yields of sterically demanding polymers to DNA, high yields and clean products were achieved for conjugation of the RAFT agent as depicted in Figure 2.

The BTPA-DNA and CPADB-DNA conjugates were further analyzed by UV-VIS, revealing pronounced shoulders at the maximum UV absorbance of the RAFT agents compared to the precursor DNA (Figure S4), and by MALDI ToF-MS (Figure 2c). As reported in the literature,[65,66] RAFT agents can undergo fragmentation *via* a six-membered transition state during the MALDI ToF-MS measurement process. As depicted in Figure 2, CPADB revealed a significantly higher tendency to fragment due to its less stable dithiobenzoic acid moiety. Monofunctionalization of the ssDNA sequences with each RAFT agent was clearly confirmed and after HPLC, purified products were isolated (Figure S5).
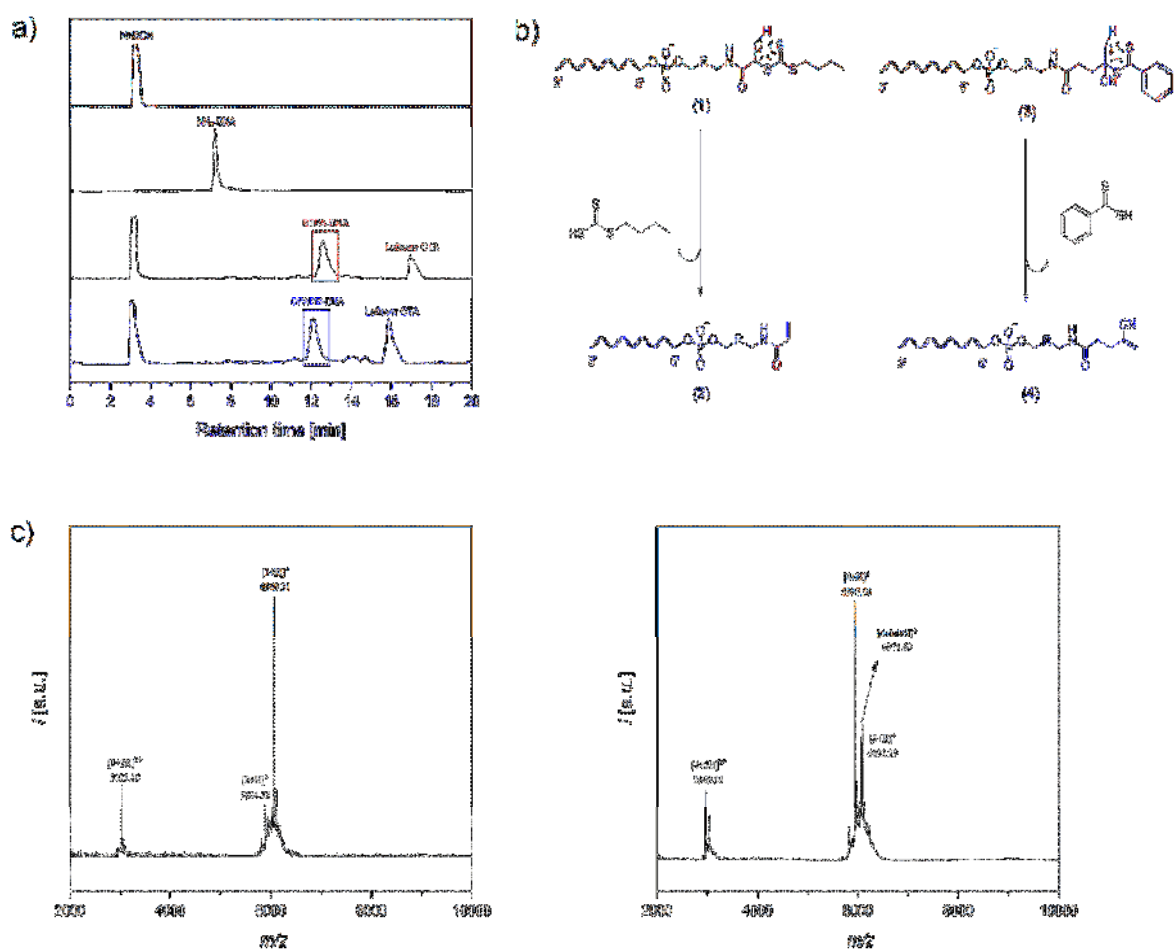
Figure 2. a) HPLC chromatograms of *N*-hydroxysuccinimide (NHSOH, line 1) and NH$_2$-ssDNA before (line 2) and after the reaction with BTPA-NHS (line 3) or CPADB-NHS (line 4), respectively. b) Schematic overview on the fragmentation reactions of BTPA-DNA (left) and CPADB-DNA (right) occurring during MALDI ToF measurements in accordance with the literature.[65,66] c) MALDI ToF mass spectra of BTPA-DNA (left) and CPADB-DNA (right). M = 3-hydroxypicolinic acid.

Photo-RAFT Model Polymerizations

Oligonucleotides are still relatively expensive and challenging to access in large milligram scales. For DNA conjugation, high ionic strength buffers are typically required and tolerance of organic solvents is limited. Therefore, in view of later applications, it is important to assess the limits of the Photo-RAFT polymerization process from ssDNA sequences in terms of reaction volume and DNA concentration in aqueous media, while maintaining a functioning RAFT equilibrium. Based on previous reports on RAFT polymerization in biological environments,[58,59] the RAFT agent concentration was set to 5 mM, which is typically considered as dilute, and polymerizations were conducted in ultralow volumes of 20 μL with water as the only solvent.

One major limitation when scaling to such small volumes is the increased sensitivity of the reaction mixture to oxygen due to the higher surface area exposed to air. Conventional deoxygenation techniques such as freeze-pump-thaw or inert gas purging are extremely challenging at these volumes. Boyer and co-workers have recently introduced an aqueous Photo-RAFT polymerization process for ultralow volumes that employs Eosin Y (EY) in the combination with ascorbic acid (AscA) as the reducing agent without the need for deoxygenation.[67] In such EY/AscA photopolymerizations, oxygen is converted into hydrogen peroxide, which subsequently reacts with ascorbic acid to form radical species capable of initiating polymerization. However, high monomer concentrations were typically employed (50 wt% monomer),[67] whereas very low concentrations are necessary for polymerization from DNA. Therefore, optimal reaction conditions for DNA-Photo-RAFT polymerization had to be identified.

Table 1. Summary of Polymers prepared by Photo-RAFT Polymerization

No.	P1	P2	P3	P4	P5	P6

Monomer ratio x[a]	200	100	400	100	80	200
RAFT agent	BTPA	BTPA	BTPA	BTPA	BTPA	CPADB
Monomer	DMA	DMA	DMA	NIPAM	OEGA	OEGMA
Irr. Time [h]	1.5	2	2	1.5	1	2.5
$M_{n,app.}$ [kDa]	12.4	6.3	18.1	11.6	11.2	13.5
$Đ$	1.15	1.21	1.14	1.22	1.36	1.40

a) Polymerizations were conducted at [Monomer]:[RAFT agent]:[EY]:[AscA] ratios of x:1:0.1:1 in water under blue light irradiation ($\lambda_{max.}$ = 470 nm, 4 mW/cm^2) at room temperature using [RAFT agent] = 5 mM. b) Apparent molecular weights and dispersities were determined by GPC with DMF as the eluent using PMMA calibration standards.

We initially assessed whether the EY/AscA system can initiate the aqueous RAFT polymerization of DMA under blue light irradiation ($\lambda_{max.}$ = 470 nm, 4 mW/cm^2, Figure S3) without prior deoxygenation using BTPA as the RAFT agent and a RAFT agent concentration of 5 mM. Employing a [DMA]:[BTPA]:[EY]:[AscA] ratio of 200:1:0.1:1 and custom-made Schlenk flasks (Figure S2), the model polymer (Table S1-**P2**) was obtained after 2 h irradiation time. However, the observed MWD was relatively broad ($Đ$ = 1.92) and exhibited tailing in the low molecular weight region while five times more concentrated conditions ([BTPA] = 25 mM) resulted in a unimodal and narrow MWD (Table S1-**P1**, $Đ$ = 1.21). These results suggested that at sufficiently high EY/AscA concentrations, the influence of molecular oxygen can be minimized. Interestingly, at low EY/AscA concentrations, the polymerization did not fail completely but rather proceeded with a significant loss in control. As such, we attempted to explore the limits by conducting the polymerization in air with substantially increased EY or AscA ratios. Nonetheless,

with a RAFT agent concentration of 5 mM, we found no notable improvement and that the MWDs still remained rather broad (Table S2-**P4**-**P7**). These observations imply that while the presence of AscA facilitated the polymerization to take place under ambient conditions, it is still insufficient to ensure good polymerization control.

Therefore, in order to improve the MWDs at low concentrations, polymerizations were additionally degassed *via* the freeze-pump-thaw technique while maintaining AscA as a reducing agent, thereby eliminating oxygen interfering with the polymerization process. Under these conditions, the Photo-RAFT polymerization of DMA afforded a polymer with narrow MWD and low dispersity (**P1**). The length of the polymer chain varied in a convenient fashion by altering the monomer to RAFT agent ratio (**P2**, **P3**). These polymerization conditions were successfully transferred to other monomers, including NIPAM (**P4**), OEGA (**P5**) and OEGMA (**P6**, SI Table 1-**P3**), and sufficient polymerization control was maintained. Noteworthy, in case the polymerization reaction was degassed *via* freeze-pump-that and EY was used without AscA, the polymerization results were not well reproducible. Most likely, varying amounts of oxygen still remained in solution after deoxygenation, which then interfered with the Photo-RAFT process. In addition, it has been reported previously that an optimal [AscA]:[RAFT agent] ratio exists for peroxide/AscA redox pairs.[68,69] For the EY/AscA system, an optimal polymerization rate was found at [AscA]:[RAFT agent] = 0.5-1 and above this ratio, the polymerization rates were significantly compromised due to undesired side reactions.[67] Therefore, in all further experiments, the [AscA]:[RAFT agent] ratio was kept constant at 1 to minimize side reactions.

DNA-Photo-RAFT Polymerization

With the optimized conditions in hand, Photo-RAFT polymerization was performed from either BTPA- or CPADB-DNA. The resulting DNA-polymer conjugates were purified by membrane filtration (MWCO = 10 kDa) in order to remove potentially unreacted precursor ssDNA sequences. GPC analysis indicated successful polymer growth from both RAFT-ssDNA sequences for every monomer (**DP1**-**DP6**). According to the GPC data, the polymer lengths were successfully varied by adjusting the monomer to RAFT-ssDNA ratio (**DP1**, **DP2**). However, compared to the model polymerizations with dispersities between 1.14 and 1.40 (Table 1), increased values between 1.6 and 2.96 were obtained when polymerizing directly from the respective RAFT-ssDNA sequence (Table 2). The observed tailing in the low molecular weight region could be due to chain transfer reactions to the ssDNA sequence, which could result in the occurrence of minor low molecular weight DNA-polymer conjugates. In addition, small shoulders of high molecular weight were observed in the case of PEGylated monomers presumably due to undesired side reactions, such as bimolecular termination events, *in situ* transesterification or chain transfer reactions to the polymers, which has been observed previously in aqueous media.[70]

Native PAGE revealed successful polymer growth from both RAFT-ssDNA sequences as new bands emerged after conducting the polymerization, indicating the formation of higher molecular weight compounds (Figure S8). These bands were relatively broad and exhibited significantly reduced mobility compared to the sharp bands of the precursor ssDNA sequence. Such diffuse bands in PAGE are relatively common, e.g., for polymer-protein conjugates[71] and reflect the polydisperse nature of the grown polymers. Hybridization of a complementary 19-mer ssDNA sequence (3'-GAGATGGTGGATGATTTTT-5') to the DNA-polymer conjugates before gel electrophoresis provided improved staining efficiency of the employed staining agent SYBR gold. The DNA-polymer conjugates of higher molecular weight exhibited slower gel movement than

the lower molecular weight conjugates and these results correspond well with the obtained GPC
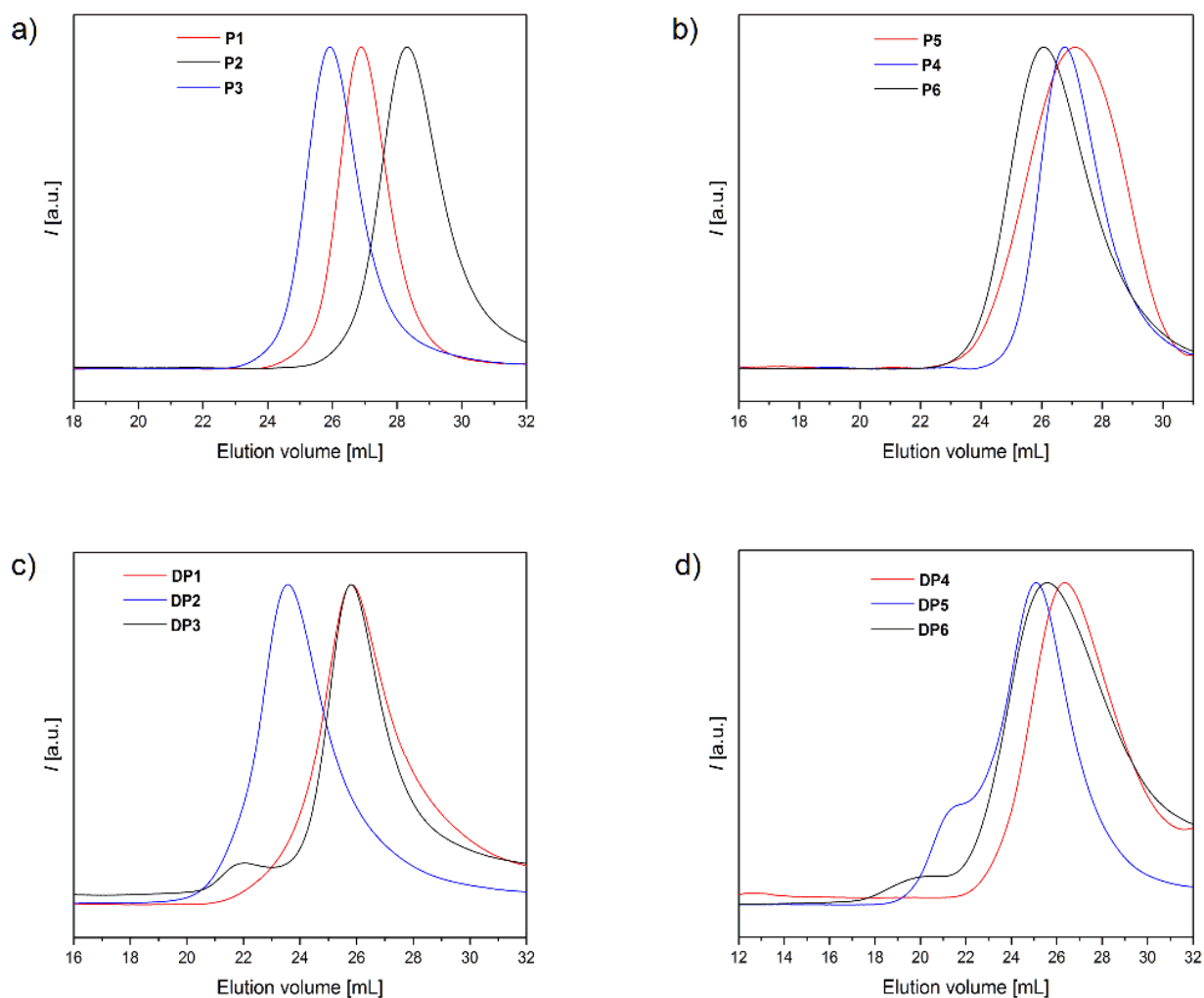
data in Figure 3.

Figure 3. GPC traces of the polymers measured in DMF with PMMA calibration standards. a)

Variation of the polymer lengths by varying monomer to RAFT agent ratio: **P1**, **P2**, **P3** according

to Table 1; b) Photo-RAFT polymerization of different monomers (NIPAM, OEGA, OEGMA):

P4, **P5**, **P6** according to Table 1; c, d) DNA-polymer conjugates of different monomers (DMA,

NIPAM, OEGA, OEGMA): **DP1**-**DP6** according to Table 2.

Table 2. Summary of DNA-Polymer Conjugates prepared by Photo-RAFT Polymerization

No.	DP1	DP2	DP3	DP4	DP5	DP6
Monomer ratio x[a]	200	500	200	80	80	200
RAFT agent	BTPA-DNA	BTPA-DNA	BTPA-DNA	BTPA-DNA	BTPA-DNA	CPADB-DNA
Monomer	DMA	DMA	NIPAM	OEGA	OEGA	OEGMA
Irr. Time [h]	2	2.5	2	1	2.33	1.5
$M_{n,app.}$ [kDa]	13.8	31.2	14.6	10.1	22.9	12.7
Đ	1.60	1.68	1.80	1.77	2.19	2.96

a) Polymerizations were conducted at [Monomer]:[RAFT-ssDNA]:[EY]:[AscA] ratios of x:1:0.1:1 in water under blue light irradiation ($\lambda_{max.}$ = 470 nm, 4 mW/cm^2) at room temperature using [RAFT-ssDNA] = 5 mM. b) Apparent molecular weights and dispersities were determined by GPC with DMF as the eluent using PMMA calibration standards.

It is a special feature of ssDNA sequences that they can be equipped with various functionalities by simple hybridization with the complementary ssDNA strand carrying the desired functionality. Rhodamine 6G-terminated complementary ssDNA was applied to the polymer solution, resulting in immediate labeling of the DNA-polymer conjugates. Fluorescence Correlation Spectroscopy[71] was then used to measure the diffusion coefficients and hydrodynamic radii of free Rhodamine 6G-terminated ssDNA and the DNA-polymer conjugates hybridized with the Rhodamine 6G-terminated ssDNA sequence. Typical FCS autocorrelation curves recorded in aqueous solution (c ≈ 40 nM) are shown in Figure 4a. The curves could be well represented by monomodal component fits (eq. S1, Supporting Information) that yielded the diffusion coefficients and consecutively the

hydrodynamic radii of the studied fluorescent species. The hydrodynamic radii substantially increased upon hybridization, evidencing the successful growth of polymer chains from RAFT-ssDNA. **DP1** and **DP4** revealed similar hydrodynamic radii as expected for polymers of similar molecular weight as determined by GPC. Importantly, **DP2** showed a significant increase in the hydrodynamic radius compared to **DP1** due to the higher molecular weight of the attached polymer, again standing in agreement with the corresponding GPC data (Figure 3).
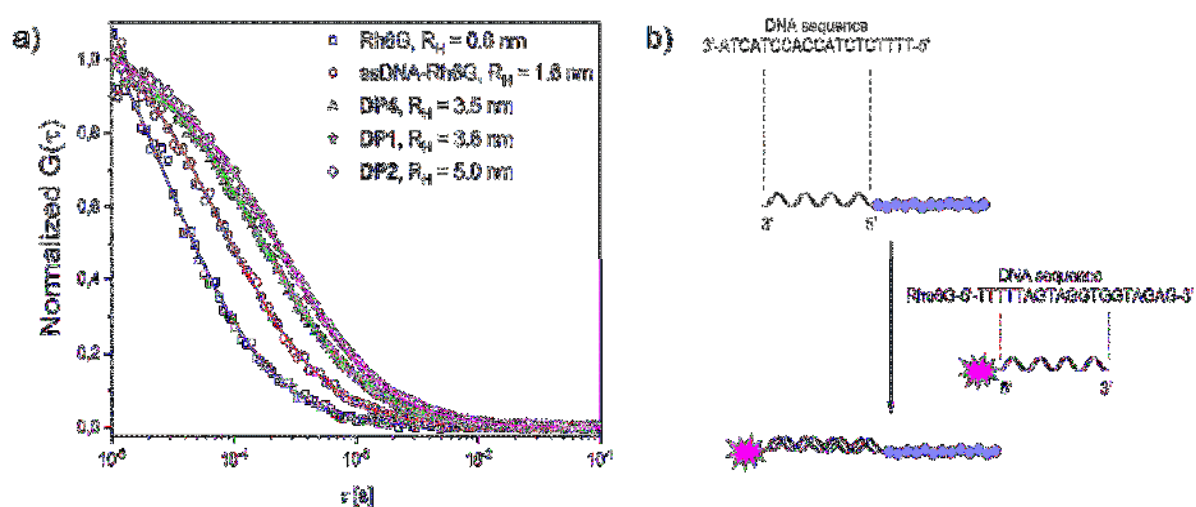

Figure 4. a) Normalized FCS autocorrelation curves (symbols) measured in aqueous solutions of Rhodamine 6G-terminated ssDNA and DNA-polymer conjugates hybridized with it. The solid lines represent the corresponding fits with eq. S1 that yielded the hydrodynamic radii of the studied fluorescent species. b) Schematic representation of the labelling of ssDNA-polymer conjugates with the complementary rhodamine 6G-terminated ssDNA sequence.

Conclusions

We introduce the first Photo-RAFT polymerization from ssDNA based on an optimized polymerization protocol. The DNA-Photo-RAFT polymerization was accomplished with four monomers yielding new DNA-polymer conjugates with varying molecular weights and acceptable

dispersities. Noteworthy, also high molecular weight conjugates above 30000 g mol^{-1} were achieved. Photo-RAFT polymerization does not require organic solvents or metal catalysts and is particularly suitable for achieving DNA-polymer conjugates in biological environments, thus complementing other synthetic and biopolymerization techniques such as ATRP and PCR. Emerging applications of this technology, e.g., for constructing more sophisticated DNA-polymer architectures controlled by light, will yield unique DNA origami-polymer nanostructures. With the current achievements in DNA upscaling, we envision many promising opportunities based on the unique characteristics of ssDNA and polymers to achieve precisely defined polymeric objects, e.g., by single chain folding where polymer shapes and functions could be controlled precisely.

ASSOCIATED CONTENT

Supporting Information. Instrumentation details and experimental setup can be found in the supporting information. NMR spectra and further characterizations are as well provided. The files are available free of charge.

AUTHOR INFORMATION

Corresponding Authors

christopher.barnerkowollik@qut.edu.au, christopher.barner-kowollik@kit.edu, david.ng@mpip-mainz.mpg.de, weil@mpip-mainz.mpg.de

Author Contributions

ABBREVIATIONS

DMA – *N,N*-dimethylacrylamide; NIPAM – *N-iso*propylacrylamide; OEGA – oligo(ethylene glycol) methyl ether acrylate; OEGMA – oligo(ethylene glycol) methyl ether methacrylate.

REFERENCES

(1) Alemdaroglu, F. E.; Herrmann, A. DNA meets synthetic polymers--highly versatile hybrid materials. *Org. Biomol. Chem.* **2007**, *5*, 1311–1320.

(2) Kwak, M.; Herrmann, A. Nucleic acid amphiphiles: synthesis and self-assembled nanostructures. *Chem. Soc. Rev.* **2011**, *40*, 5745–5755.

(3) Schnitzler, T.; Herrmann, A. DNA block copolymers: functional materials for nanoscience and biomedicine. *Acc. Chem. Res.* **2012**, *45*, 1419–1430.

(4) Peng, L.; Wu, C.; You, M.; Han, D.; Chen, Y.; Fu, T.; Ye, M.; Tan, W. Engineering and Applications of DNA-Grafting Polymer Materials. *Chem. Sci.* **2013**, *4*, 1928–1938.

(5) Surin, M. From nucleobase to DNA templates for precision supramolecular assemblies and synthetic polymers. *Polym. Chem.* **2016**, *7*, 4137–4150.

(6) Agarwal, N. P.; Matthies, M.; Gür, F. N.; Osada, K.; Schmidt, T. L. Block Copolymer Micellization as a Protection Strategy for DNA Origami. *Angew. Chem., Int. Ed.* **2017**, *56*, 5460–5464.

(7) Ponnuswamy, N.; Bastings, M. M. C.; Nathwani, B.; Ryu, J. H.; Chou, L. Y. T.; Vinther, M.; Li, W. A.; Anastassacos, F. M.; Mooney, D. J.; Shih, W. M. Oligolysine-based coating protects DNA nanostructures from low-salt denaturation and nuclease degradation. *Nat. Commun.* **2017**, *8*, 15654.

(8) Chidchob, P.; Edwardson, T. G. W.; Serpell, C. J.; Sleiman, H. F. Synergy of Two Assembly Languages in DNA Nanostructures: Self-Assembly of Sequence-Defined Polymers on DNA Cages. *J. Am. Chem. Soc.* **2016**, *138*, 4416–4425.

(9) Trinh, T.; Liao, C.; Toader, V.; Barłóg, M.; Bazzi, H. S.; Li, J.; Sleiman, H. F. DNA-imprinted polymer nanoparticles with monodispersity and prescribed DNA-strand patterns. *Nat. Chem.* **2018**, *10*, 184–192.

(10) Serpell, C. J.; Edwardson, T. G. W.; Chidchob, P.; Carneiro, K. M. M.; Sleiman, H. F. Precision polymers and 3D DNA nanostructures: emergent assemblies from new parameter space. *J. Am. Chem. Soc.* **2014**, *136*, 15767–15774.

(11) Knudsen, J. B.; Liu, L.; Bank Kodal, A. L.; Madsen, M.; Li, Q.; Song, J.; Woehrstein, J. B.; Wickham, S. F. J.; Strauss, M. T.; Schueder, F. Vinther, J.; Krissanaprasit, A.; Gudnason, D.; Abbotsford Smith, A. A.; Ogaki, R.; Zelikin, A. N.; Besenbacher, F.; Birkedal, V.; Yin, P.; Shih, W. M.; Jungmann, R.; Dong M.; Gothelf K. V. Routing of individual polymers in designed patterns. *Nat. Nanotechnol.* **2015**, *10*, 892–898.

(12) Krissanaprasit, A.; Madsen, M.; Knudsen, J. B.; Gudnason, D.; Surareungchai, W.; Birkedal, V.; Gothelf, K. V. Programmed Switching of Single Polymer Conformation on DNA Origami. *ACS Nano* **2016**, *10*, 2243–2250.

(13) Li, Z.; Zhang, Y.; Fullhart, P.; Mirkin, C. A. Reversible and Chemically Programmable Micelle Assembly with DNA Block-Copolymer Amphiphiles. *Nano Lett.* **2004**, *4*, 1055–1058.

(14) Ding, K.; Alemdaroglu, F. E.; Börsch, M.; Berger, R.; Herrmann, A. Engineering the structural properties of DNA block copolymer micelles by molecular recognition. *Angew. Chem., Int. Ed.* **2007**, *46*, 1172–1175.

(15) Chien, M.-P.; Rush, A. M.; Thompson, M. P.; Gianneschi, N. C. Programmable shape-shifting micelles. *Angew. Chem., Int. Ed.* **2010**, *49*, 5076–5080.

(16) Rodríguez-Pulido, A.; Kondrachuk, A. I.; Prusty, D. K.; Gao, J.; Loi, M. A.; Herrmann, A. Light-Triggered Sequence-Specific Cargo Release from DNA Block Copolymer-Lipid Vesicles. *Angew. Chem., Int. Ed.* **2013**, *125*, 1042–1046.

(17) Banga, R. J.; Krovi, S. A.; Narayan, S. P.; Sprangers, A. J.; Liu, G.; Mirkin, C. A.; Nguyen, S. T. Drug-Loaded Polymeric Spherical Nucleic Acids: Enhancing Colloidal Stability and Cellular Uptake of Polymeric Nanoparticles through DNA Surface-Functionalization. *Biomacromolecules* **2017**, *18*, 483–489.

(18) Alemdaroglu, F. E.; Alemdaroglu, N. C.; Langguth, P.; Herrmann, A. DNA Block Copolymer Micelles – A Combinatorial Tool for Cancer Nanotechnology. *Adv. Mater.* **2008**, *20*, 899–902.

(19) Cui, P.-F.; Zhuang, W.-R.; Qiao, J.-B.; Zhang, J.-L.; He, Y.-J.; Luo, C.-Q.; Jin, Q.-R.; Xing, L.; Jiang, H.-L. Histone-inspired biomimetic polymeric gene vehicles with excellent biocompatibility and enhanced transfection efficacy. *Polym. Chem.* **2016**, *7*, 7416–7426.

(20) Alemdaroglu, F. E.; Ding, K.; Berger, R.; Herrmann, A. DNA-templated synthesis in three dimensions: Introducing a micellar scaffold for organic reactions. *Angew. Chem., Int. Ed.* **2006**, *45*, 4206–4210.

(21) Kwak, M.; Minten, I. J.; Anaya, D.-M.; Musser, A. J.; Brasch, M.; Nolte, R. J. M.; Müllen, K.; Cornelissen, J. J. L. M.; Herrmann, A. Virus-like particles templated by DNA micelles: a general method for loading virus nanocarriers. *J. Am. Chem. Soc.* **2010**, *132*, 7834–7835.

(22) Hong, F.; Zhang, F.; Liu, Y.; Yan, H. DNA Origami: Scaffolds for Creating Higher Order Structures. *Chem. Rev.* **2017**, *117*, 12584–12640.

(23) Wilner, O. I.; Willner, I. Functionalized DNA nanostructures. *Chem. Rev.* **2012**, *112*, 2528–2556.

(24) Tokura, Y.; Jiang, Y.; Welle, A.; Stenzel, M. H.; Krzemien, K. M.; Michaelis, J.; Berger, R.; Barner-Kowollik, C.; Wu, Y.; Weil, T. Bottom-Up Fabrication of Nanopatterned Polymers on DNA Origami by In Situ Atom-Transfer Radical Polymerization. *Angew. Chem., Int. Ed.* **2016**, *55*, 5692–5697.

(25) Tokura, Y.; Harvey, S.; Chen, C.; Wu, Y.; Ng, D. Y. W.; Weil, T. Fabrication of Defined Polydopamine Nanostructures by DNA Origami-Templated Polymerization. *Angew. Chem., Int. Ed.* **2018**, *57*, 1587–1591.

(26) Watson, K. J.; Park, S.-J.; Im, J.-H.; Mirkin, C. A. DNA–Block Copolymer Conjugates. *J. Am. Chem. Soc.* **2001**, *123*, 5592–5593.

(27) Rochambeau, D. de; Barłóg, M.; Edwardson, T. G. W.; Fakhoury, J. J.; Stein, R. S.; Bazzi, H. S.; Sleiman, H. F. "DNA–Teflon" sequence-controlled polymers. *Polym. Chem.* **2016**, *7*, 4998–5003.

(28) Wilks, T. R.; Bath, J.; Vries, J. W. de; Raymond, J. E.; Herrmann, A.; Turberfield, A. J.; O'Reilly, R. K. "Giant surfactants" created by the fast and efficient functionalization of a DNA tetrahedron with a temperature-responsive polymer. *ACS Nano* **2013**, *7*, 8561–8572.

(29) Averick, S.; Paredes, E.; Li, W.; Matyjaszewski, K.; Das, S. R. Direct DNA conjugation to star polymers for controlled reversible assemblies. *Bioconjugate Chem.* **2011**, *22*, 2030–2037.

(30) Oishi, M.; Nagatsugi, F.; Sasaki, S.; Nagasaki, Y.; Kataoka, K. Smart polyion complex micelles for targeted intracellular delivery of PEGylated antisense oligonucleotides containing acid-labile linkages. *ChemBioChem* **2005**, *6*, 718–725.

(31) Oishi, M.; Sasaki, S.; Nagasaki, Y.; Kataoka, K. pH-responsive oligodeoxynucleotide (ODN)-poly(ethylene glycol) conjugate through acid-labile beta-thiopropionate linkage: preparation and polyion complex micelle formation. *Biomacromolecules* **2003**, *4*, 1426–1432.

(32) Safak, M.; Alemdaroglu, F. E.; Li, Y.; Ergen, E.; Herrmann, A. Polymerase Chain Reaction as an Efficient Tool for the Preparation of Block Copolymers. *Adv. Mater.* **2007**, *19*, 1499–1505.

(33) Jeong, J. H.; Kim, S. H.; Kim, S. W.; Park, T. G. Polyelectrolyte complex micelles composed of c-raf antisense oligodeoxynucleotide-poly(ethylene glycol) conjugate and poly(ethylenimine): effect of systemic administration on tumor growth. *Bioconjugate Chem.* **2005**, *16*, 1034–1037.

(34) Jeong, J. H.; Kim, S. W.; Park, T. G. Novel intracellular delivery system of antisense oligonucleotide by self-assembled hybrid micelles composed of DNA/PEG conjugate and cationic fusogenic peptide. *Bioconjugate Chem.* **2003**, *14*, 473–479.

(35) Jeong, J. H.; Park, T. G. Novel Polymer−DNA Hybrid Polymeric Micelles Composed of Hydrophobic Poly(d , l -lactic- co -glycolic Acid) and Hydrophilic Oligonucleotides. *Bioconjugate Chem.* **2001**, *12*, 917–923.

(36) Wilks, T. R.; O'Reilly, R. K. Efficient DNA-Polymer Coupling in Organic Solvents: A Survey of Amide Coupling, Thiol-Ene and Tetrazine-Norbornene Chemistries Applied to Conjugation of Poly(N-Isopropylacrylamide). *Sci. Rep.* **2016**, *6*, 39192.

(37) Sowwan, M.; Faroun, M.; Mentovich, E.; Ibrahim, I.; Haboush, S.; Alemdaroglu, F. E.; Kwak, M.; Richter, S.; Herrmann, A. Polarizability of DNA block copolymer nanoparticles observed by electrostatic force microscopy. *Macromol. Rapid Commun.* **2010**, *31*, 1242–1246.

(38) Braunecker, W. A.; Matyjaszewski, K. Controlled/living radical polymerization: Features, developments, and perspectives. *Prog. Polym. Sci.* **2007**, *32*, 93–146.

(39) Matyjaszewski, K. Atom Transfer Radical Polymerization (ATRP): Current Status and Future Perspectives. *Macromolecules* **2012**, *45*, 4015–4039.

(40) Matyjaszewski, K.; Xia, J. Atom Transfer Radical Polymerization. *Chem. Rev.* **2001**, *101*, 2921–2990.

(41) Moad, G.; Rizzardo, E.; Thang, S. H. Living Radical Polymerization by the RAFT Process. *Aust. J. Chem.* **2005**, *58*, 379.

(42) Moad, G.; Rizzardo, E.; Thang, S. H. Radical addition–fragmentation chemistry in polymer synthesis. *Polymer* **2008**, *49*, 1079–1131.

(43) Lou, X.; Wang, C.; He, L. Core-shell Au nanoparticle formation with DNA-polymer hybrid coatings using aqueous ATRP. *Biomacromolecules* **2007**, *8*, 1385–1390.

(44) Lou, X.; Lewis, M. S.; Gorman, C. B.; He, L. Detection of DNA point mutation by atom transfer radical polymerization. *Anal. Chem.* **2005**, *77*, 4698–4705.

(45) Lou, X.; He, L. DNA-accelerated atom transfer radical polymerization on a gold surface. *Langmuir* **2006**, *22*, 2640–2646.

(46) He, P.; Zheng, W.; Tucker, E. Z.; Gorman, C. B.; He, L. Reversible addition-fragmentation chain transfer polymerization in DNA biosensing. *Anal. Chem.* **2008**, *80*, 3633–3639.

(47) He, P.; He, L. Synthesis of surface-anchored DNA-polymer bioconjugates using reversible addition-fragmentation chain transfer polymerization. *Biomacromolecules* **2009**, *10*, 1804–1809.

(48) Pan, X.; Lathwal, S.; Mack, S.; Yan, J.; Das, S. R.; Matyjaszewski, K. Automated Synthesis of Well-Defined Polymers and Biohybrids by Atom Transfer Radical Polymerization Using a DNA Synthesizer. *Angew. Chem., Int. Ed.* **2017**, *56*, 2740–2743.

(49) Averick, S. E.; Dey, S. K.; Grahacharya, D.; Matyjaszewski, K.; Das, S. R. Solid-Phase Incorporation of an ATRP Initiator for Polymer-DNA Biohybrids. *Angew. Chem., Int. Ed.* **2014**, *126*, 2777–2782.

(50) Treat, N. J.; Sprafke, H.; Kramer, J. W.; Clark, P. G.; Barton, B. E.; Read de Alaniz, J.; Fors, B. P.; Hawker, C. J. Metal-free atom transfer radical polymerization. *J. Am. Chem. Soc.* **2014**, *136*, 16096–16101.

(51) Theriot, J. C.; Lim, C.-H.; Yang, H.; Ryan, M. D.; Musgrave, C. B.; Miyake, G. M. Organocatalyzed atom transfer radical polymerization driven by visible light. *Science* **2016**, *352*, 1082–1086.

(52) Pearson, R. M.; Lim, C.-H.; McCarthy, B. G.; Musgrave, C. B.; Miyake, G. M. Organocatalyzed Atom Transfer Radical Polymerization Using N-Aryl Phenoxazines as Photoredox Catalysts. *J. Am. Chem. Soc.* **2016**, *138*, 11399–11407.

(53) Semsarilar, M.; Perrier, S. 'Green' reversible addition-fragmentation chain-transfer (RAFT) polymerization. *Nat. Chem.* **2010**, *2*, 811–820.

(54) Xu, J.; Jung, K.; Atme, A.; Shanmugam, S.; Boyer, C. A robust and versatile photoinduced living polymerization of conjugated and unconjugated monomers and its oxygen tolerance. *J. Am. Chem. Soc.* **2014**, *136*, 5508–5519.

(55) Xu, J.; Jung, K.; Corrigan, N. A.; Boyer, C. Aqueous photoinduced living/controlled polymerization: tailoring for bioconjugation. *Chem. Sci.* **2014**, *5*, 3568.

(56) Delzenne, G.; Toppet, S.; Smets, G. Photopolymerization of acrylamide. I. Formation of the initiating redox system. *J. Polym. Sci.* **1960**, *48*, 347–355, DOI: 10.1002/pol.1960.1204815034.

(57) Xu, J.; Shanmugam, S.; Duong, H. T.; Boyer, C. Organo-photocatalysts for photoinduced electron transfer-reversible addition–fragmentation chain transfer (PET-RAFT) polymerization. *Polym. Chem.* **2015**, *6*, 5615–5624.

(58) Niu, J.; Lunn, D. J.; Pusuluri, A.; Yoo, J. I.; O'Malley, M. A.; Mitragotri, S.; Soh, H. T.; Hawker, C. J. Engineering live cell surfaces with functional polymers via cytocompatible controlled radical polymerization. *Nat. Chem.* **2017**, *9*, 537–545.

(59) Tucker, B. S.; Coughlin, M. L.; Figg, C. A.; Sumerlin, B. S. Grafting-From Proteins Using Metal-Free PET–RAFT Polymerizations under Mild Visible-Light Irradiation. *ACS Macro Lett.* **2017**, *6*, 452–457.

(60) Beaucage, S. L.; Iyer, R. P. Advances in the Synthesis of Oligonucleotides by the Phosphoramidite Approach. *Tetrahedron* **1992**, *48*, 2223–2311.

(61) Qiu, X.-P.; Winnik, F. M. Facile and Efficient One-Pot Transformation of RAFT Polymer End Groups via a Mild Aminolysis/Michael Addition Sequence. *Macromol. Rapid Commun.* **2006**, *27*, 1648–1653.

(62) Xu, J.; He, J.; Fan, D.; Wang, X.; Yang, Y. Aminolysis of Polymers with Thiocarbonylthio Termini Prepared by RAFT Polymerization: The Difference between Polystyrene and Polymethacrylates. *Macromolecules* **2006**, *39*, 8616–8624.

(63) Willcock, H.; O'Reilly, R. K. End group removal and modification of RAFT polymers. *Polym. Chem.* **2010**, *1*, 149–157.

(64) Lockett, M. R.; Phillips, M. F.; Jarecki, J. L.; Peelen, D.; Smith, L. M. A tetrafluorophenyl activated ester self-assembled monolayer for the immobilization of amine-modified oligonucleotides. *Langmuir* **2008**, *24*, 69–75.

(65) Charles, L.; Lejars, M.; Margaillan, A.; Bressy, C. Fragmentation pathways of methacrylic homopolymers with labile trialkylsilyl ester side-groups—A mass spectrometric investigation of the RAFT process. *Int. J. Mass Spectrom.* **2012**, *311*, 31–39.

(66) Oehlenschlaeger, K. K.; Mueller, J. O.; Heine, N. B.; Glassner, M.; Guimard, N. K.; Delaittre, G.; Schmidt, F. G.; Barner-Kowollik, C. Light-induced modular ligation of conventional RAFT polymers. *Angew. Chem., Int. Ed.* **2013**, *52*, 762–766.

(67) Yeow, J.; Chapman, R.; Xu, J.; Boyer, C. Oxygen tolerant photopolymerization for ultralow volumes. *Polym. Chem.* **2017**, *8*, 5012–5022.

(68) Lv, Y.; Liu, Z.; Zhu, A.; An, Z. Glucose oxidase deoxygenation–redox initiation for RAFT polymerization in air. *J. Polym. Sci. A* **2017**, *55*, 164–174.

(69) Kitagawa, M.; Tokiwa, Y. Polymerization of vinyl sugar ester using ascorbic acid and hydrogen peroxide as a redox reagent. *Carbohydr. Polym.* **2006**, *64*, 218–223.

(70) Robinson, K. L.; Khan, M. A.; Paz Báñez, M. V. de; Wang, X. S.; Armes, S. P. Controlled Polymerization of 2-Hydroxyethyl Methacrylate by ATRP at Ambient Temperature. *Macromolecules* **2001**, *34*, 3155–3158.

(71) Bontempo, D.; Maynard, H. D. Streptavidin as a macroinitiator for polymerization: in situ protein-polymer conjugate formation. *J. Am. Chem. Soc.* **2005**, *127*, 6508–6509.

TOC

Photo-RAFT from DNA